BIOCHEMISTRY
including biophysical chemistry & molecular biology

Article

pubs.acs.org/biochemistry

Voltage-Driven Ca^{2+} Binding at the L-Type Ca^{2+} Channel Triggers Cardiac Excitation–Contraction Coupling Prior to Ca^{2+} Influx

Liron S. Gez,[†] Yamit Hagalili,[†] Asher Shainberg,[‡] and Daphne Atlas*,[†]

[†]Department of Biological Chemistry, Institute of Life Sciences, The Hebrew University of Jerusalem, Jerusalem 91904, Israel
[‡]The Mina and Everard Goodman Faculty of Life Sciences, Bar-Ilan University, Ramat-Gan 52900, Israel

Supporting Information

ABSTRACT: The activation of the ryanodine Ca^{2+} release channels (RyR2) by the entry of Ca^{2+} through the L-type Ca^{2+} channels (Cav1.2) is believed to be the primary mechanism of excitation–contraction (EC) coupling in cardiac cells. This proposed mechanism of Ca^{2+}-induced Ca^{2+} release (CICR) cannot fully account for the lack of a termination signal for this positive feedback process. Using Cav1.2 channel mutants, we demonstrate that the Ca^{2+}-impermeable $\alpha_1$1.2/L775P/T1066Y mutant introduced through lentiviral infection into neonate cardiomyocytes triggers Ca^{2+} transients in a manner independent of Ca^{2+} influx. In contrast, the $\alpha_1$1.2/L775P/T1066Y/4A mutant, in which the Ca^{2+}-binding site of the channel was destroyed, supports neither the spontaneous nor the electrically evoked contractions. Ca^{2+} bound at the channel selectivity filter appears to initiate a signal that is conveyed directly from the channel pore to RyR2, triggering contraction of cardiomyocytes prior to Ca^{2+} influx. Thus, RyR2 is activated in response to a conformational change in the L-type channel during membrane depolarization and not through interaction with Ca^{2+} ions diffusing in the junctional gap space. Accordingly, termination of the RyR2 activity is achieved when the signal stops upon the return of the L-channel to the resting state. We propose a new model in which the physical link between Cav1.2 and RyR2 allows propagation of a conformational change induced at the open pore of the channel to directly activate RyR2. These results highlight Cav1.2 as a signaling protein and provide a mechanism for terminating the release of Ca^{2+} from RyR2 through protein–protein interactions. In this model, the L-type channel is a master regulator of both initiation and termination of EC coupling in neonate cardiomyocytes.

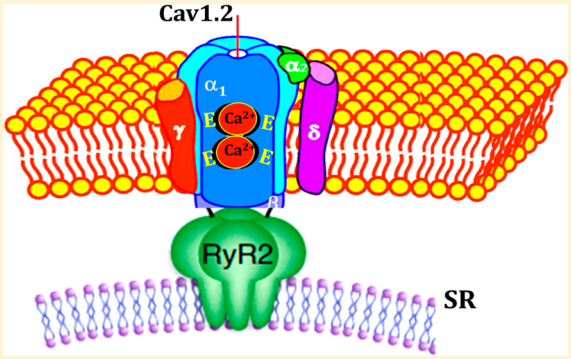

In skeletal muscle, a physical linkage between L-type Ca^{2+} channels (Cav1.2) and RyR1 is believed to be the primary mechanism of excitation–contraction (EC) coupling.[1] In contrast, in cardiac muscle, the physical interaction between Cav1.2 and ryanodine Ca^{2+} release channels (RyR2) plays a minimal role in initiating EC coupling.[2−4]

Several studies have shown that RyR gating in intact ventricular myocytes is sensitive to structural changes induced by binding of BayK 8644 to Cav1.2, in a manner independent of Ca^{2+} influx.[5−7] A cytosolic peptide that links segments II and III of the $\alpha_1$1.2 subunit of the L-type Ca^{2+} channel inhibits the RyR opening and EC coupling without altering calcium currents or SR Ca^{2+} content.[4] The competition of the recombinant II–III peptide with the native $\alpha_1$1.2 subunit of Cav1.2 was further supported by single-channel measurements showing interactions of selective peptides of the $\alpha_1$1.2 II–III loop with the native RyR2 channel. These results indicate that cardiac Cav1.2, like skeletal Cav1.1, has the potential for a physical–conformational coupling to RyR.[8,9] It was suggested, however, that the role of a physical linkage between the two proteins in EC coupling is minimal because Cav1.2 in the heart is expressed in relatively small amounts[10] and is not targeted to positions opposite RyR2.[11]

The widely accepted mechanism of EC coupling in the heart is mediated by Ca^{2+}-induced Ca^{2+} release (CICR). However, CICR poses a paradox of control, because this positive feedback process lacks a termination signal.[12,13] Nevertheless, the local control theory of CICR theory seems to explain most of the CICR characteristics.[14−19] It states that the release of Ca^{2+} from RyR2 is controlled by the influx of Ca^{2+} through immediately adjacent Cav1.2 and not by the elevated global Ca^{2+} concentration throughout the cytosol.

Here we examined whether during Ca^{2+} binding at the pore and prior to Ca^{2+} influx, Cav1.2 could initiate EC coupling. This mechanism, which is permitted by the physical coupling between Cav1.2 and RyR2, suggests that a conformational change in the channel is transmitted directly to RyR2, while termination of the release of Ca^{2+} from the SR is reached with the return of the channel from an activated to a resting state.

We focused mainly on evaluating the contribution of the initial Ca^{2+} binding at the selectivity filter of the pore of the L-type Ca^{2+} channel, and its role in initiating Cav1.2–RyR2

Received: August 20, 2012
Revised: November 13, 2012
Published: November 13, 2012

dx.doi.org/10.1021/bi301124a | *Biochemistry* 2012, 51, 9658–9666

signaling prior to the entry of Ca^{2+} into the cell. We reveal an unexpected and novel mode of interaction previously shown in neuroendorine cells,[20] which could represent the prevailing communication of Cav1.2 with RyR2 in the neonatal heart.

MATERIALS AND METHODS

The complete cDNA of the $\alpha_1$1.2 subunit (rabbit) (dN60-del1773; GenBank entry X15539) was kindly donated by N. Qin and L. Birnbaumer (University of North Carolina, Chapel Hill, NC), the pCSC-SP-PW-GFP vector by I. Verma, the α1 subunit in-frame 5′ to the coding region of a modified green fluorescent protein (GFP) by M. Grabner, and $\alpha_1$1.2/L775P by S. Hering. The constructs with the GFP channel made for expression in *Xenopus* oocytes,[20] which contained the T1066Y mutation or the L775P and T1066Y mutations, were inserted into lentiviral vector pCSC-SP-PW-GFP at the PstI and BamHI sites, generating the corresponding $\alpha_1$1.2/T1066Y and $\alpha_1$1.2/L775P/T1066Y viral vectors. The construct with the GFP channel, which carried the L775P and T1066Y mutations, was mutagenized at positions E393A, E736A, E1145A, and E1446A using the appropriate primers and inserted into lentiviral vector pCSC-SP-PW-GFP at the PstI and BamHI sites, generating the $\alpha_1$1.2/L775P/T1066Y/4A vector.

Nifedipine (Sigma) was dissolved in dimethyl sulfoxide (DMSO) (final concentrations of <0.1%). Results are expressed as means ± the standard error of the mean (SEM) for the indicated number (n) of myocytes, and p values of <0.01 and <0.001 were considered significant (Student's t test).

Preparation of Heart Cultures. The animals were purchased from Harlan Laboratories (Jerusalem, Israel). The experiments were conducted in accordance with the guidelines of the Animal Care and Use Committee of Bar-Ilan University, with the Guide for the Care and Use of Laboratory Animals published by the U.S. National Institutes of Health.

Sprague-Dawley rat hearts (2−3 days old) were removed under sterile conditions and washed three times in PBS to remove excess blood cells. The hearts were minced into small fragments and then gently agitated in RDB, a solution of proteolytic enzymes prepared from fig-tree extract (Biological Institute, Ness-Ziona, Israel). RDB was diluted 1:100 in Ca^{2+}- and Mg^{2+}-free PBS at 25 °C and incubated with the heart fragments for several cycles of 10 min each, as previously described.[21] Dulbecco's modified Eagle's medium, supplemented with 10% inactivated horse serum (Biological Industries, Kibbutz Beit Haemek, Israel) and 0.5% chick embryo extract, was added to the supernatant containing a suspension of dissociated cells. The mixture was centrifuged at 300g for 5 min. The supernatant was discarded, and the cells were resuspended. The cell suspension was diluted to a density of 1.0×10^6 cells/mL, and 1.5 mL of the suspension was placed in 35 mm plastic culture dishes or glass coverslips coated with collagen and/or gelatin. The cultures were incubated in a humidified atmosphere of 5% CO_2 and 95% air at 37 °C. A confluent monolayer exhibiting spontaneous contractions developed within 2 days. The experiments were performed on 4−6-day-old cardiomyocyte cultures.

Intracellular Ca^{2+} Measurements. Cellular calcium images of individual cardiomyocytes were obtained from heart cultures preloaded with 3 μM Indo-1 and 1.5 μM pluronic acid for 30 min in glucose-enriched PBS at 25 °C, as previously described.[22] Indo-1 is excited at 340 nm; the emitted light is split by a dichroic mirror to two photomultipliers (Hamamatsu Corp.) with input filters at 410 and 490 nm. The fluorescent signals at 410 and 490 nm acquired every 10 ms were fed to a CAPLAN program written by D. Kaplan from the Biological Institute (Ness-Ziona, Israel). The increase in the intensity of the fluorescence ratio of 410 nm to 490 nm is proportional to the increase in $[Ca^{2+}]_i$. The amplitude, time to peak, time to 90% decay, and rate of rise (dR/dt) of the derived $[Ca^{2+}]_i$ transients were determined with IonWizard.

Infection of Cardiomyocytes with Lentivirus. *Lentivirus Packaging.* Viruses were produced by calcium phosphate transfection of HEK293T cells. Cells were cultured in DMEM containing 10% FBS, 100 units/mL penicillin/streptomycin, and 2 mM glutamine at a confluency of 60−80% in a 10 cm dish. The medium was changed 1 day postculture, and 6 h later cells were cotransfected with the lentiviral vector (amounts per dish) (8.92 μg), packaging vectors pRSV-REV and pMDL (2.21 and 5.78 μg, respectively), and the vesicular somatitis G glycoprotein (VSVG) expression vector (3.12 μg). The total amount of DNA was 20 μg per plate. The transfection solution consisted of HBSS buffer (100 mM HEPES, 13.5 mM NaCl, 5 mM KCl, 5.5 mM D-glucose, 1.9 mM Na_2HPO_4, and 2.5 mM $CaCl_2$). $CaCl_2$ was added last while the solution was being mixed. After 20 min at room temperature, the solution (1 mL) was added dropwise to each plate and incubated overnight at 37 °C. Virus was collected from the culture supernatant in two time intervals. The first was 40 h post-transfection, after which fresh medium was added to the cells and the virus was collected again, 50 h post-transfection. The supernatants were combined and centrifuged at 1800 rpm for 10 min, and cell waste was discarded. Virus was filtered through a 0.45 μm filter and concentrated by ultracentrifugation for 2 h at 25000 rpm and 4 °C. Ultracentrifugation tubes contained 10 mL of 10% sucrose for extra filtration. The supernatant was discarded. The pellet was resuspended in medium, kept for 1 h at 4 °C, resuspended, and incubated for 30 min at 4 °C. Finally, the virus was resuspended in medium, divided into tubes, and stored at −70 °C.

The virus titer was determined by infecting 293T cells at a density of 2×10^5 cells/well in six-well dishes at serial dilutions (1:1−1:32). Forty-eight hours postinfection, the infected cells expressed GFP and a robust evaluation of the percent of GFP-expressing cells determined the dilution required in the experimental infection.

Lentiviral Transduction in Rat Neonatal Cardiomyocytes. One to days postculture, the cardiomyocytes were incubated with lentivirus diluted in 500 μL of DMEM with 2% serum. The plates were incubated for 3 h at 37 °C in 5% CO_2 and gently shaken every 5 min. Then 1 mL of medium with 10% serum was added to each plate, and the cells were incubated for 48 h until the day of the experiment.

Expression in *Xenopus* Oocytes and cRNA Injection. Preparation of *Xenopus laevis* oocytes, cRNA injection, and electrophysiological measurements were conducted essentially as described previously.[20]

Calcium currents (I_{Ca}) and lithium currents (I_{Li}) through voltage-gated Ca^{2+} channels were recorded in *Xenopus* oocytes at 22 °C, 5 days after injection using the standard two-microelectrode voltage clamp.[23]

To minimize Ca^{2+}-activated Cl^- currents, oocytes were injected with 5 mM BAPTA (final concentration) prior to recordings. Membrane currents were recorded by a two-electrode voltage-clamp method using a TEV-200A amplifier (Dagan).[23] Current traces were leak-subtracted online with Clampex 8.2, and channel activation rates were analyzed by

dx.doi.org/10.1021/bi301124a | *Biochemistry* 2012, 51, 9658−9666

applying a monoexponential fit (Axon Instruments, Foster City, CA) to the current traces in the relevant ranges.

Data Presentation and Statistical Analysis. For *Xenopus* oocytes, peak currents were analyzed with Clampfit 9.0 and transferred as an ASCI file to an Excel worksheet (Microsoft Inc.). Data were averaged for each group of oocytes, and the standard error (SE) was determined. Data are presented as means ± SE. Statistical significance relative to the control group in each experiment was determined by a Student's t test with Excel.

Parameters of Ca^{2+} Transients. A train of pulses with a base level B describes the Ca^{2+} transient. Each pulse starts at time t_1 from level y_o, where the previous pulse ends, rises according to capacitor charging with time constant τ_2 until time t_2, and then falls according to capacitor discharging with time constant τ_3. A curve-fitting algorithm was used to obtain all parameters in the following expression:

$$f(t) = B + \begin{cases} y_0 e^{t_1 - t/\tau_1} & t \le t_1 \\ y_0 + c(1 - e^{t_1 - t/\tau_2}), & t_1 \le t \le t_2 \\ (y_0 + A)e^{t_2 - t/\tau_3}, & t \ge t_2 \end{cases}$$

in which the pulse amplitude (A) is given by the equation

$$A = c(1 - e^{t_1 - t_2/\tau_2})$$

The initial rise and decay rates are obtained from the time derivatives at times t_1 and t_2, yielding c/τ_2 and $(y_0 + A)/\tau_3$, respectively.

The data points used to fit each pulse are selected in the following way: A very rough smoothing (using spline approximation) is performed on all data points. Local minima and maxima of the smoothed curves are identified. For a given pulse, all points starting from the midtime between the previous minimum and the previous maximum, and ending at the next minimum, are selected (the correct time for pulse beginning and peak are to be extracted from the fit). Each pulse is then analyzed independently.

RESULTS

A Ca^{2+}-Impermeable Cav1.2 Mutant Mediates Spontaneous Contractions of Cardiomyocytes in a Manner Independent of Ca^{2+} Entry. The goal of this work is to establish the ability of rat neonatal cardiomyocytes to trigger, in response to voltage and binding of Ca^{2+} at Cav1.2, release of Ca^{2+} from the SR prior to Ca^{2+} influx. To this end, we used lentivirus-encoded Cav1.2 mutants. All of the mutants also carried a second mutation, T1066Y, rendering them resistant to the selective Cav1.2 blocker, nifedipine (Nif). We first tested the Nif sensitivity of spontaneous contractions (Ca^{2+} transients) in control cells. Contractions were monitored by the fluorescence ratio at 410 nm to 490 nm of the fluorescent Ca^{2+}-sensitive dye Indo-1 (Figure 1A).[22] As shown in panels A and B of Figure 1, 8 μM Nif completely eliminated Ca^{2+} transients, blocking spontaneous contractions. Nifedipine abolishes contractions by selectively binding to the L-type calcium channels, ruling out contraction triggered by other sources of Ca^{2+} entry. Thus, 8 μM Nif allowed us to study the effects of exogenous lentivirus-encoded Cav1.2 Nif-resistant mutants in cardiac cells when the endogenous channels are silent.

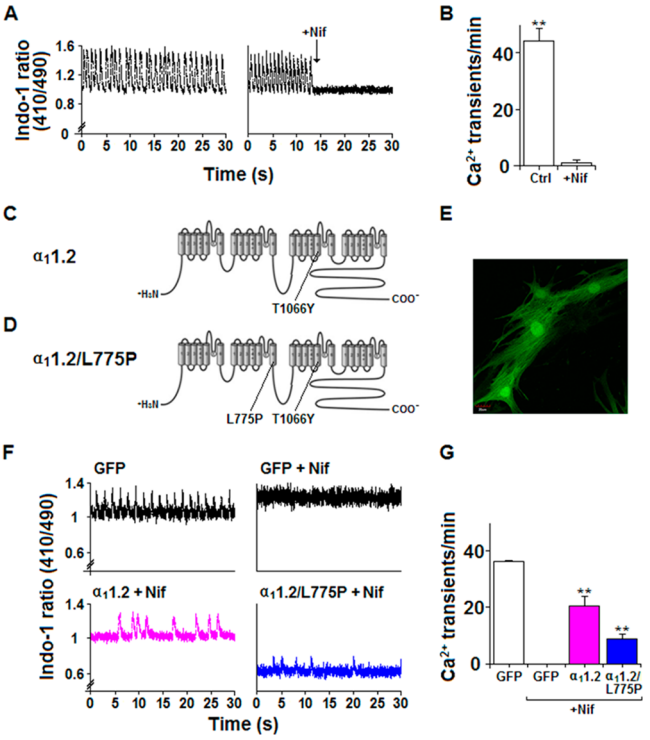

Figure 1. Ca^{2+} transients elicited in cardiomyocytes through the activation of Ca^{2+}-impermeable L-type channels (Cav1.2). (A) Traces of Ca^{2+} transients elicited spontaneously in the presence and absence of 8 μM nifedipine (Nif) are depicted as the ratio of Indo-1 fluorescence at 410nm to 490 nm. (B) Frequency of Ca^{2+} transients in the absence and presence of Nif. Data are shown as means ± SEM and analyzed by a Student's t test. $^{**}p < 0.001$ ($n = 20$). (C and D) Schematic view of (C) $\alpha_1$1.2/T1066Y harboring the T1066Y mutation that renders the channel Nif-resistant and (D) $\alpha_1$1.2/L775P/T1066Y harboring both the L775P mutation that blocks current influx and Nif-resistant T1066Y mutation. (E) Confocal image of cardiomyocytes visualized 3 days after infection (400×). (F) Traces (top) of Ca^{2+} transients elicited spontaneously in cells infected with lentivirus vector carrying GFP, in the absence and presence of 8 μM Nif. Ca^{2+} transients (bottom) of Nif-resistant functional the $\alpha_1$1.2/T1066Y channel subunit ($\alpha_1$1.2) or Nif-resistant $\alpha_1$1.2/L775P/T1066Y ($\alpha_1$1.2/L775P) in the presence of 8 μM Nif. (G) Frequency of Ca^{2+} transients in the absence and presence of Nif. Data are shown as means ± SEM and analyzed by a Student's t test. $^{**}p < 0.001$ ($n = 20$) (see Table 1).

To explore Ca^{2+} influx that is independent of Cav1.2−RyR interactions, we employed a Ca^{2+}-impermeable Cav1.2 mutant, which does not transport Ca^{2+}.[24] In applying this strategy, we prevent the entry of Ca^{2+} through Cav1.2 without altering other pathways or changing the physiological conditions of the cells. This approach is more selective and less harmful compared to membrane permeabilization, or using chelating reagents to omit Ca^{2+} from the extracellular medium. We used the Nif-resistant $\alpha_1$1.2 pore subunit of the L-type channel $\alpha_1$1.2/T1066Y and the Ca^{2+}-impermeable $\alpha_1$1.2/L775P/T1066Y mutant (Figure 1C,D). The Ca^{2+}-impermeable mutant exhibits voltage sensitivity and binds Ca^{2+} at the channel pore during channel activation.[20,25] Cardiac myocytes were infected with the pCSC lentiviral vector carrying the GFP fused to the functional $\alpha_1$1.2/T1066Y Nif-resistant mutant, or Ca^{2+}-impermeable Nif-resistant $\alpha_1$1.2/L775P/T1066Y mutant. Cells expressing the GFP-tagged viruses were visualized using confocal microscopy (Figure 1E).

dx.doi.org/10.1021/bi301124a | *Biochemistry* 2012, 51, 9658−9666

Spontaneous contractions were monitored as Ca^{2+} transients by Indo-1 ratiometric $[Ca^{2+}]_i$ imaging. The frequency of Ca^{2+} transients in cells infected with GFP alone was 35 ± 4 transients/min (Figure 1F and Table S1 of the Supporting Information), compared to that of uninfected cells control cells (Ctrl), 44 ± 4.5 transients/min (Figure 1A and Table S1 of the Supporting Information). As in control cells, Ca^{2+} transients were not elicited in GFP-infected cells in the presence of 8 μM Nif (Figure 1F, top right).

Next, spontaneous Ca^{2+} transients were triggered in the presence of 8 μM Nif, in cardiomyocytes infected with the Nif-resistant $\alpha_1$1.2/T1066Y subunit, depicted as $\alpha_1$1.2 in all the figures, or the Nif-resistant $\alpha_1$1.2/L775P/T1066Y Ca^{2+}-impermeable mutant, depicted as $\alpha_1$1.2/L775P in all the figures (Figure 1F,G). The frequency of Ca^{2+} transients in cardiomyocytes infected with a functional Nif-resistant channel was lower (20.5 ± 3.4 transients/min) than in GFP-infected cells [36.7 ± 0.3 transients/min (Table S2 of the Supporting Information)]. A weaker signal was expected for infected cells than for noninfected cells. Remarkably, however, the expression of the Ca^{2+}-impermeable $\alpha_1$1.2/L775P/T1066Y mutant was sufficient to drive prominent Ca^{2+} transients [8.8 ± 1.8 transients/min (Figure 1F,G and Table S2 of the Supporting Information)]. Because the endogenous channels are Nif-sensitive, only ~4% of the control GFP-infected cells responded with Ca^{2+} transients, in the presence of Nif, compared to 77% of the Nif-resistant $\alpha_1$1.2/T1066Y-infected cells. There was little difference between the $\alpha_1$1.2/T1066Y and Ca^{2+}-impermeable $\alpha_1$1.2/L775P/T1066Y mutant, for which 64% of the cells displayed Ca^{2+} transients (Table S2 of the Supporting Information).

To exclude unrelated effects due to overexpression of channels in the cardiomyocytes, like interaction and/or clustering of endogenous channels with the exogenous channels, we monitored spontaneous contractions in the cells prior to adding Nif. The frequency of spontaneous Ca^{2+} transients monitored before adding Nif to $\alpha_1$1.2/T1066Y-infected cells (42.9 ± 4.8 transients/min; n = 31), was similar to the control (44.1 ± 4.5 transients/min; n = 19) and slightly higher than that of GFP-infected cells (33.3 ± 0.3 transients/cell: n = 6). The frequency observed in $\alpha_1$1.2/L775P/T1066Y-infected cells prior to adding Nif was lower (29 ± 4.4 transients/min; n = 22).

The Ca^{2+}-Impermeable Channel Supports Electrical Stimulation Contractions of Cardiomyocytes. Next, we tested whether electrical activation of the Ca^{2+}-impermeable $\alpha_1$1.2/L775P/T1066Y channel triggers the release of Ca^{2+} from the SR. Cardiomyocytes were preloaded with Indo-1 for 60 min and electrically stimulated (20−50 V) for 10 ms at a frequency of 0.6 Hz (Figure 2). The frequency of Ca^{2+} release in uninfected cardiomyocytes (44 ± 4.5 transients/min) was reduced to 1.1 ± 1 transients/min in the presence of 8 μM Nif (Figure 2A and Table S3 of the Supporting Information). Then $\alpha_1$1.2/T1066Y- or $\alpha_1$1.2/L775P/T1066Y-infected cells were stimulated in the presence of 8 μM Nif. The voltage-activated Ca^{2+}-impermeable channel $\alpha_1$1.2/L775P/T1066Y elicited Ca^{2+} transients at a frequency (37.3 ± 2.7 transients/min) similar to that of the $\alpha_1$1.2/T1066Y channel (28.8 ± 5.2 transients/min). These values were also similar to the Ca^{2+} transient frequency in GFP-infected cells (36.8 ± 3.8 transients/min) obtained in the absence of Nif (Figure 2B and Table S3 of the Supporting Information).

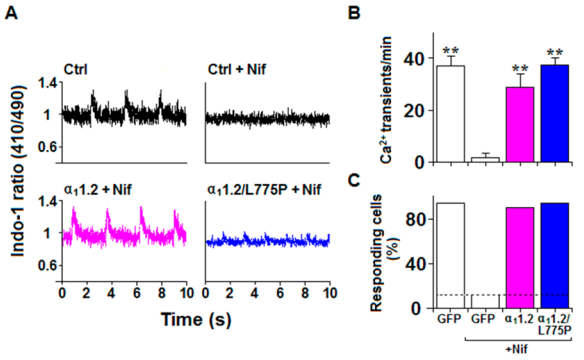

Figure 2. Cardiac excitation−contraction coupling mediated by a Ca^{2+}-impermeable $\alpha_1$1.2/L775P mutant. (A) Representative 410 nm to 490 nm traces elicited in control cardiomyocytes in response to electrical stimulation in the absence (left) and presence (right) of 8 μM Nif. (B) Representative 410 nm to 490 nm plots elicited from cardiomyocytes infected with the Nif-resistant functional $\alpha_1$1.2 T1066Y subunit ($\alpha_1$1.2) and the Nif-resistant $\alpha_1$1.2/L775P/T1066Y ($\alpha_1$1.2/L775P) mutant. (C) Frequency of Ca^{2+} transients in the presence and absence of Nif. Data are shown as means ± SEM and analyzed by a Student's t test. $^{**}p < 0.001$ (n = 20) (see Table 1).

The similar frequency observed in Ca^{2+}-permeable and Ca^{2+}-impermeable channels strongly indicates that Cav1.2−RyR2 coupling could be triggered in a manner independent of Ca^{2+} entry. Most of the cardiomyocytes infected with $\alpha_1$1.2/T1066Y (90%) or $\alpha_1$1.2/L775P/T1066Y (94%, responded to cell stimulation in the presence of Nif, as compared with 12% of the control cells (Figure 2C and Table S2 of the Supporting Information). The frequency of Ca^{2+} transients in the same cells, stimulated prior to adding Nif, was 34.8 ± 6.2 transients/min (n = 10) for $\alpha_1$1.2/T1066Y, was 43.1 ± 3.5 transients/min (n = 40) for $\alpha_1$1.2/L775P/T1066Y, and was similar to that of control cells with 34.4 ± 5.2 transients/sec (n = 10).

Kinetic Parameters of Ca^{2+} Transients in Lentivirus-Infected Cardiomyocytes. We evaluated the kinetic parameters of Ca^{2+} transients, monitoring the amplitude, area, and rates of rise and decay (Figure 3A). The amplitude of spontaneous Ca^{2+} transients was reduced by 30% in $\alpha_1$1.2 T1066Y-infected cells and 50% in $\alpha_1$1.2/L775P/T1066Y-infected cells, compared to that of GFP-infected cells (Figure 3B and Table 1). Also the area under the curve, which like amplitude is directly related to the amount of Ca^{2+} released, was not affected in the $\alpha_1$1.2/T1066Y-infected cells but was reduced by 50% in $\alpha_1$1.2/L775P/T1066Y-infected cells, compared to that of GFP-infected cells (Figure 3B and Table 1). In contrast, no significant difference in the rate of rise in $\alpha_1$1.2/T1066Y or $\alpha_1$1.2/L775P/T1066Y mutants was observed, compared to that of GFP-infected cells (Figure 3B and Table S4 of the Supporting Information). The decay time, which represents the removal of Ca^{2+} from the cytoplasm by the SR, sarcolemal Ca-ATPase, and the sodium−calcium exchanger, was not affected (Figure 3 and Table 1).

Similar to spontaneous Ca^{2+} transients, a significant reduction in peak fluorescence (~40%) and area was recorded in $\alpha_1$1.2/L775P/T1066Y-infected cells during membrane depolarization, with no apparent change in the rate of rise or decay (Figure 3C and Table 1). These results support the view that conformational coupling rather than Ca^{2+} entry plays a major role in initiating Ca^{2+} transients. The smaller amplitude and area of the Ca^{2+} transient triggered in $\alpha_1$1.2/L775P/T1066Y-infected cells indicate a lower level of release of Ca^{2+}

dx.doi.org/10.1021/bi301124a | Biochemistry 2012, 51, 9658−9666

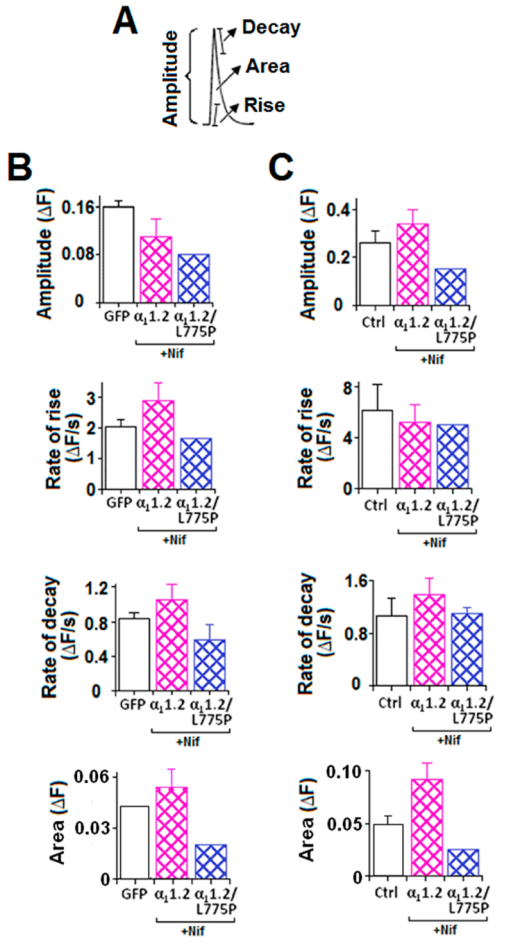

Figure 3. Parameters of Ca^{2+} transients, amplitude, rise time, and decay time. (A) Parameters of Ca^{2+} transients were evaluated using the curve-fitting algorithm (Materials and Methods). (B) Representation of the mean Ca^{2+} transient amplitude, rate of rise, rate of decay, and area under the curve of Ca^{2+} transients spontaneously elicited in cardiomyocyte cultures infected with GFP (white), functionally Nif insensitive $\alpha_1$1.2/T1066Y ($\alpha_1$1.2) (pink), or $\alpha_1$1.2/L775P/T1066Y ($\alpha_1$1.2/L775P) (blue). (C) Representation of the mean Ca^{2+} transient amplitude evoked by electrical stimulation in control cardiomyocytes (white) or cardiomyocytes infected with $\alpha_1$1.2/T1066Y ($\alpha_1$1.2) (pink) or $\alpha_1$1.2/L775P/T1066Y ($\alpha_1$1.2/L775P) (blue). *p < 0.01; **p < 0.01.

from the SR. It could result from a reduction in the number of excitation units,[26] caused by the aberrant coupling of the mutated channel to RyR2. It also could indicate that even though Ca^{2+} entry is not essential for triggering Ca^{2+} transients or modifying their kinetics, it is supportive of the generation of a full-scale signal.

Direct conformational coupling between two adjacent proteins, where Cav1.2 directly controls RyR2 signaling through physical coupling, is faster than CICR and provides a highly regulated means for terminating the release of Ca^{2+} from the SR. Specific functional interactions between the Cav1.2 cytosolic domains and RyR2 were shown in ferret ventricular myocytes[27] or in SR vesicles from sheep heart using lipid bilayers.[8]

Selective Mutations at the Selectivity Filter of the L-Type Calcium Channel. Previous studies have demonstrated that SR Ca^{2+} release in ventricular myocytes does not occur in the absence of extracellular Ca^{2+},[28] or in the presence of selective Ca^{2+} channel blockers such as Cd^{2+}.[29,30] Because Ca^{2+} and Cd^{2+} bind at the channel selectivity filter, we examined whether the apparent Ca^{2+} dependency of cardiac contraction prior to Ca^{2+} influx results from occupancy of the channel pore. The Cav1.2 Ca^{2+}-binding site is composed of four glutamate residues, E393, E736, E1145, and E1446, called the EEEE motif[31−34] (Figure 4). Site-directed mutagenesis has shown that Ca^{2+} binding affinity is greatly attenuated by single and double substitutions in the EEEE locus and is eliminated by quadruple alanine (AAAA), glutamine (QQQQ), or aspartate (DDDD) substitutions.[35] These mutations do not seem to strongly affect the pore structure, using the substituted-cysteine accessibility method.[36−38] The EEEE Ca^{2+}-binding site at the pore can bind a single Ca^{2+} ion with high affinity (K_d < 1 μM) and multiple ions with low affinity (K_d = 13.4 mM)[37,38] (Figure 4A,B). During channel opening, the high-affinity Ca^{2+} binding site is converted from a single Ca^{2+}-occupied site into a low-affinity multiple-Ca^{2+}-occupied site. It has been suggested that in the conversion from a single-ion pore to a multiple-ion pore, passing from a nonconductive to a conductive state, the channel undergoes a conformational change, schematically shown in panels A and B of Figure 4. On the basis of triggering catecholamine[20,41] or release of insulin[42] independent of Ca^{2+} entry, this switch was proposed to represent a signal transduction mechanism in which the Ca^{2+} channel acts as a signaling protein in a manner independent of conducting Ca^{2+} into the cell.[39,40,43] To examine whether Ca^{2+} binding at the channel pore is essential for eliciting Ca^{2+} transients prior to Ca^{2+} entry, we used a Ca^{2+}-impermeable channel mutated at the Ca^{2+} EEEE binding motif.

Mutating the Ca^{2+} Binding Motif of the Cardiac L-Type Channel Prevents Cardiomyocyte Contractions. We mutated the EEEE site and verified that the quadruple-alanine $\alpha_1$1.2/AAAA mutant was incapable of supporting Ca^{2+} or Li^+ currents when expressed in *Xenopus* oocytes[35] (Figure

Table 1. Kinetic Parameters of Ca^{2+} Transients

	amplitude (ΔF)	rate of rise (ΔF/s)	rate of decay (ΔF/s)	area (ΔF)
		Spontaneous Contractions		
GFP	0.16 ± 0.01 (6)	2.03 ± 0.23 (6)	0.84 ± 0.06 (6)	0.04 ± 0.00 (6)
$\alpha_1$1.2/T1066Y[a]	0.11 ± 0.03 (6)	2.88 ± 0.57 (28)	1.06 ± 0.17 (28)	0.05 ± 0.01 (28)
$\alpha_1$1.2/L775P/T1066Y[a]	0.08 ± 0.01 (7)[b]	1.63 ± 0.44 (14)	0.59 ± 0.18 (14)	0.02 ± 0.00 (14)
		Stimulated Contractions		
control	0.26 ± 0.05 (15)	6.11 ± 2.06 (15)	1.07 ± 0.26 (15)	0.06 ± 0.01 (11)
$\alpha_1$1.2/T1066Y[a]	0.34 ± 0.06 (9)	5.21 ± 1.39 (9)	1.39 ± 0.26 (9)	0.11 ± 0.02 (9)
$\alpha_1$1.2/L775P/T1066Y[a]	[c]0.15 ± 0.02 (27)	5.0 ± 0.73 (27)	1.1 ± 0.1 (27)	0.03 ± 0.00 (22)

[a]In the presence of 8 μM Nif. [b]p < 0.001. [c]p < 0.01.

dx.doi.org/10.1021/bi301124a | *Biochemistry* 2012, 51, 9658−9666

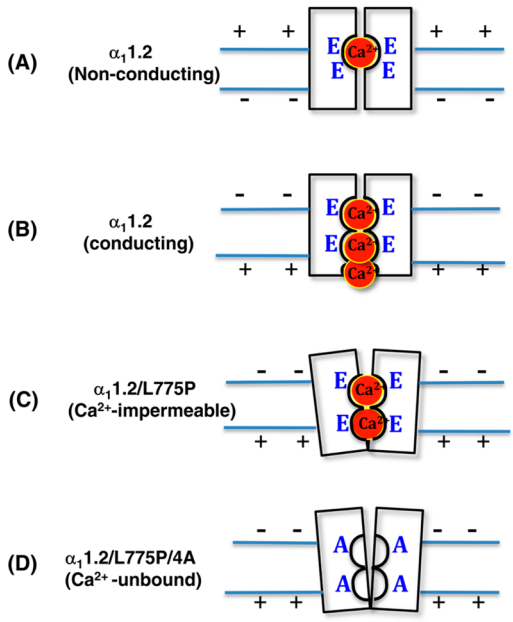

Figure 4. Schematic presentation of the $\alpha_1$1.2 subunit and its mutants. (A) The single-cation-occupied pore of the channel subunit represents a close nonconducting channel. The EEEE motif is colored blue. All channel subunits harbor the T1066Y mutation, which renders them Nif-resistant. (B) During depolarization, the channel becomes cation-conductive upon saturation of a second low-affinity Ca^{2+}-binding site within the channel pore.[38] (C) Mutating $\alpha_1$1.2 via the L775P mutation renders the channel Ca^{2+}-impermeable[24] without removing its ability to bind Ca^{2+}.[20] (D) Mutating four Glu (E) residues to Ala (see Figure 5) prevents binding of Ca^{2+} at the channel pore.

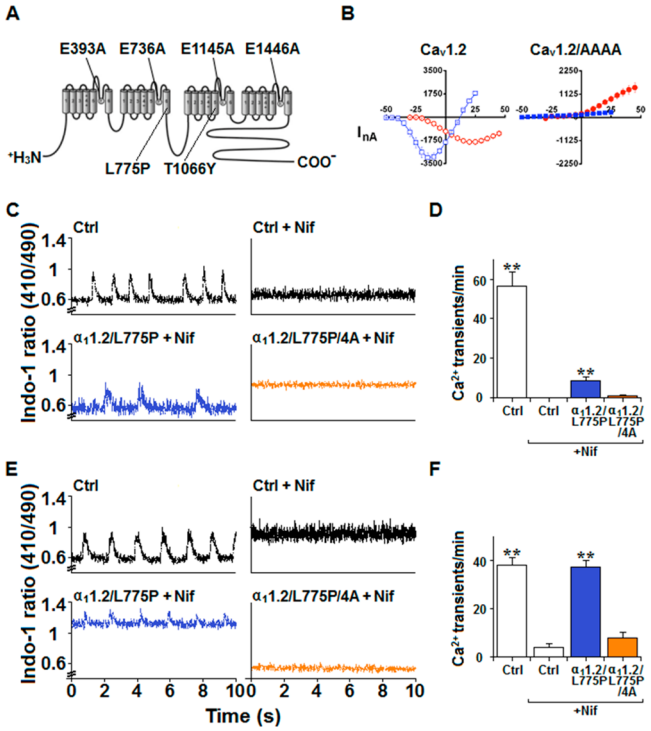

Figure 5. Mutated Ca^{2+} binding site of Cav1.2/L775P that impedes induction of Ca^{2+} transients. (A) $\alpha_1$1.2 subunit mutated at four Glu (E) residues composing the Ca^{2+} binding site at the selectivity filter. (B) Current–voltage relationship of Cav1.2 and the Cav1.2/4A mutant expressed in *Xenopus* oocytes. Inward currents were elicited from a holding potential of −80 mV to various test potentials at 5 mV increments in response to a 1200 ms test pulse: I_{Ca} currents colored red and I_{Li} currents colored blue. (C) Representative 410 nm to 490 nm traces spontaneously elicited in control cells in the presence and absence of 8 μM Nif (top), $\alpha_1$1.2/L775P/T1066Y-infected cells ($\alpha_1$1.2/L77P) (bottom left), or $\alpha_1$1.2/L775P/T1066Y/4A-infected cells ($\alpha_1$1.2/L775P4A) (bottom right), in the presence of 8 μM Nif. (D) Frequency of spontaneously evoked Ca^{2+} transients in control and infected cells. Data are shown as means ± SEM and analyzed by a Student's *t* test. $^{**}p < 0.001$ (n = 20). (E) Representative 410 nm to 490 nm traces elicited in response to electric stimulation in control cells in the absence and presence of 8 μM Nif (top), $\alpha_1$1.2/L775P/T1066Y-infected cells ($\alpha_1$1.2/L77P) (bottom left), or $\alpha_1$1.2/L775P/T1066Y/4A-infected cells ($\alpha_1$1.2/L77P4A) (bottom right) in the presence of 8 μM Nif. (F) Frequency of depolarization-evoked Ca^{2+} transients in control and infected cells. Data are shown as means ± SEM and analyzed by a Student's *t* test. $^{**}p < 0.001$ (n = 20).

5B). Then the quadruple (4A) mutation was inserted into the Ca^{2+}-impermeable $\alpha_1$1.2/L775P/T1066Y subunit, and the new mutant, $\alpha_1$1.2/L775P/T1066Y/4A, which is Ca^{2+}-impermeable, Nif-resistant, and unable to bind Ca^{2+} at the pore, was inserted into the lentivirus vector. Spontaneous (Figure 5C,D) and stimulated Ca^{2+} transients (Figure 5E,F) were examined in cardiomyocytes infected with this vector in the presence of 8 μM Nif and compared to those of control uninfected cells and cells infected with the $\alpha_1$1.2/L775P/T1066Y mutant.

As shown by the Indo-1 fluorescence ratio (410 nm to 490 nm), no spontaneous release of Ca^{2+} from intracellular stores was detected in cells infected with $\alpha_1$1.2/L775P/T1066Y/4A (Figure 5C,E). The infected cells that were stimulated prior to the addition of Nif displayed even higher levels of Ca^{2+} release (72.3 ± 4.4 transients/min; n = 18) compared to control cells (44.1 ± 4.5 transients/min; n = 19). During electrical stimulation, the frequency of Ca^{2+} transients elicited by $\alpha_1$1.2/L775P/T1066Y/4A-infected cardiomyocytes (0.8 ± 0.8 transients/min) was not significantly different from the frequency in control cells stimulated in the presence of Nif (1.13 ± 1.13 transients/min). Prior to the addition of Nif, the frequency of Ca^{2+} transients in electrically stimulated $\alpha_1$1.2/L775P/4A-infected cells was 43.5 ± 9.6 transients/min (n = 4), which was similar to that of control cells, 34.3 ± 5.2 transients/min (n = 10). Only 27% of the $\alpha_1$1.2/L775P/T1066Y/4A-infected cells responded, compared to 94% of the cells infected with $\alpha_1$1.2/L775P/T1066Y (Figure 5D,F and Table S2 of the Supporting Information). Hence, the $\alpha_1$1.2/L775P/T1066Y/4A mutant, displaying no capacity to bind Ca^{2+}, appeared to have lost its ability to communicate with RyR2.

DISCUSSION

In this study, we demonstrate that a Ca^{2+}-impermeable L-type Ca^{2+} channel triggers spontaneous and electrically stimulated contractions in cardiomyocytes. Although the mechanism of spontaneous beating is different from that of myofilament contractions, both are sensitive to nifedipine, indicating a strong dependency on Cav1.2 activation. Our results show that the initiation of contractions is dependent on Ca^{2+} occupying the pore of the channel, independent of Ca^{2+} influx. Thus, EC coupling requires Ca^{2+} binding at the Ca^{2+}-binding site of the open channel and depends on voltage, which is indispensable for channel opening. In contrast, Ca^{2+} influx is not a mandatory component of the initiation of EC coupling. Substantial conformational changes induced during cation binding at the channel selectivity filter have been reported for K^+ channels[44] and Ca^{2+} channels.[39,41]

dx.doi.org/10.1021/bi301124a | *Biochemistry* 2012, 51, 9658–9666

It is commonly accepted that direct Cav1.2−RyR2 coupling does not contribute significantly to EC coupling in the heart.[4] Our results suggest that the physical and functional interactions between Cav1.2 and RyR2[8,9,27] allows transmission of a signal initiated during Ca^{2+} binding at the channel pore. Thus, a conformational change induced during Ca^{2+} binding is transmitted most likely via the cardiac $\alpha_1$1.2 II−III loop directly to RyR2, similar to signaling catecholamine release in neuroendocrine cells.[20,40] We suggest that the physical coupling of Cav1.2 and RyR allows a Ca^{2+} influx-independent signaling mechanism in the heart. Possibly, the weak physical interactions between Cav1.2 and RyR2 in cardiac cells are modified during channel activation and become crucial for EC coupling. Li and Bers have shown a bidirectional cross talk between Cav1.2 and RyR2 by a Cav1.2 II−III loop peptide that through competing with the endogenous cytosolic $\alpha_1$1.2 II−III domain inhibited the resting Ca^{2+} sparks in ferret ventricles[27] (see also refs 5−7).

Our results suggest that a change in conformation induced at the channel during voltage perturbation involves binding of Ca^{2+} to the EEEE motif, which directly signals RyR2, to promote contractions in the neonatal heart. Perhaps specific for the neonatal heart, in which the SR is immature and the contribution of CICR to cardiac contraction is weak, it would be interesting to study the importance of this interaction in facilitating adult cardiac EC coupling.

Mutating the four glutamate residues at the selectivity filter, which constitute the Ca^{2+}-binding site of the channel, abolishes Ca^{2+} binding at the channel pore. Our results show that a Ca^{2+}-impermeable mutant that, also lost its capacity to bind Ca^{2+}, when introduced by lentivirus into cardiomyocytes was unable to elicit the release of Ca^{2+} from the SR.

The instant communication between Cav1.2 and RyR2 that is disrupted in the Ca^{2+}-unbound quadruply (4A) mutated EEEE motif further confirms that Ca^{2+} bound at the open pore is essential for Cav1.2−RyR2 coupling, indicating a major role of the channel in triggering EC coupling.

Cd^{2+} ions that bind with high affinity and compete with Ca^{2+} for binding to the EEEE locus[38,45] would be expected to disrupt EC coupling like the AAAA quadruple mutation (4A). Indeed, EC coupling was significantly inhibited by Cd^{2+} ions.[29,30]

Our results are consistent with previous studies showing that Cav1.2 is the only protein that can gate the fast release of Ca^{2+} from the SR within the range of the action potential,[46] and that depolarization per se without extracellular Ca^{2+} is not sufficient to evoke EC coupling.[13,47−49] Because binding at the pore of the Ca^{2+}-impermeable Cav1.2 is sufficient to elicit contractions in the absence of Ca^{2+} inflow, extracellular Ca^{2+} is required mainly to allow binding at the channel pore and not inside the cell.

Furthermore, the proposed signaling model suggests that termination of EC coupling is dependent on the Ca^{2+}-conducting conformation of Cav1.2. Accordingly, EC coupling should terminate when depolarization stops and the non-conducting state of the closed channel no longer transmits a signal to RyR2, or other potential associated proteins.[50,51] Such a direct mechanism provides for the rapid and high-fidelity on−off signaling of cardiac contractions. Our results are also consistent with studies in which release of SR Ca^{2+} was terminated either by elevating depolarization toward the reversal potential of the L-type current[15] or by repolarization.[48,52,53] A direct voltage regulation of release of Ca^{2+} from the SR was also suggested in voltage-clamp experiments using Cav1.2 selective blockers.[54]

In conclusion, our results emphasize the importance of Ca^{2+} binding at the selectivity filter of the L-type Ca^{2+} channel as the trigger of EC coupling. They highlight the channel as a Ca^{2+}-binding protein that acts as a molecular switch, triggering the release of Ca^{2+} from the SR through RyR2, in a manner independent of Ca^{2+} influx. Initiating cardiac contractions requires extracellular Ca^{2+} for saturating the low-affinity Ca^{2+}-binding site at the channel pore, prior to Ca^{2+} entry. The conversion of Cav1.2 to a conductive state triggers Ca^{2+} contractions also when Cav1.2 is Ca^{2+}-impermeable, namely in the absence of Ca^{2+} entry. However, when the channel loses its ability to bind Ca^{2+}, EC coupling is stopped. These data strongly suggest that EC coupling is initiated by the channel that propagates a signal during Ca^{2+} binding at the pore to RyR2, in a manner independent of Ca^{2+} permeation. The initial interaction of Ca^{2+} ions at the pore, largely ignored as a potential signaling event, is essential for triggering the release of Ca^{2+} from the SR, highlighting Cav1.2 as a signaling protein and a master regulator of EC coupling. Signaling through a direct interaction between Cav1.2 and RyR2 raises additional questions related to further characterization of the Cav1.2−RyR2 interaction interface,[8,27] the structural organization of Cav1.2 vis-à-vis RyR2,[27] and finally defining a cardiac-specific Cav1.2−RyR2 link shared with Cav1−RyR1 signaling, and with Cav1.2 coupling to the exocytotic proteins in secretory systems.[20,25,40]

■ ASSOCIATED CONTENT

Supporting Information

Ratios of the number of contracting cells to the total number of cells within the different groups (Table S1), frequencies of spontaneously induced Ca^{2+} transients in cardiomyocytes (Table S2), and frequencies of voltage-induced Ca^{2+} transients in cardiomyocytes (Table S3). This material is available free of charge via the Internet at http://pubs.acs.org.

■ AUTHOR INFORMATION

Corresponding Author

*Department of Biological Chemistry, Institute of Life Sciences, The Hebrew University of Jerusalem, Jerusalem 91904, Israel. Phone: 972-2-658-5406. Fax: 972-2-651-2958. E-mail: datlas@vms.huji.ac.il.

Author Contributions

D.A. conceived and designed the experiments. L.S.G. and Y.H. performed the experiments. L.S.G., Y.H., A.S., and D.A. analyzed the data. A.S. contributed reagents, materials, and analysis tools. D.A. wrote the paper.

Funding

Supported by the H. L. Lautherbach Fund (D.A.).

Notes

The authors declare no competing financial interest.

■ ACKNOWLEDGMENTS

We thank Dr. Smadar Schatz for the curve-fitting algorithm and Dr. Shoshana Kline and Dr. Michael Trus for their critical reading of this paper prior to submission.

■ REFERENCES

(1) Flucher, B. E., and Franzini-Armstrong, C. (1996) Formation of junctions involved in excitation-contraction coupling in skeletal and cardiac muscle. *Proc. Natl. Acad. Sci. U.S.A. 93*, 8101−8106.

(2) Fabiato, A. (1985) Time and calcium dependence of activation and inactivation of calcium-induced release of calcium from the sarcoplasmic reticulum of a skinned canine cardiac Purkinje cell. *J. Gen. Physiol. 85*, 247−289.
(3) Bers, D. M. (2002) Cardiac excitation-contraction coupling. *Nature 415*, 198−205.
(4) Wier, W. G., and Balke, C. W. (1999) Ca^{2+} release mechanisms, Ca^{2+} sparks, and local control of excitation-contraction coupling in normal heart muscle. *Circ. Res. 85*, 770−776.
(5) McCall, E., Hryshko, L. V., Stiffel, V. M., Christensen, D. M., and Bers, D. M. (1996) Possible functional linkage between the cardiac dihydropyridine and ryanodine receptor: Acceleration of rest decay by Bay K 8644. *J. Mol. Cell. Cardiol. 28*, 79−93.
(6) Satoh, H., Katoh, H., Velez, P., Fill, M., and Bers, D. M. (1998) Bay K 8644 increases resting Ca^{2+} spark frequency in ferret ventricular myocytes independent of Ca influx: Contrast with caffeine and ryanodine effects. *Circ. Res. 83*, 1192−1204.
(7) Katoh, H., Schlotthauer, K., and Bers, D. M. (2000) Transmission of information from cardiac dihydropyridine receptor to ryanodine receptor: Evidence from BayK 8644 effects on resting Ca^{2+} sparks. *Circ. Res. 87*, 106−111.
(8) Dulhunty, A. F., Curtis, S. M., Cengia, L., Sakowska, M., and Casarotto, M. G. (2004) Peptide fragments of the dihydropyridine receptor can modulate cardiac ryanodine receptor channel activity and sarcoplasmic reticulum Ca^{2+} release. *Biochem. J. 379*, 161−172.
(9) Dulhunty, A. F., Karunasekara, Y., Curtis, S. M., Harvey, P. J., Board, P. G., and Casarotto, M. G. (2005) The recombinant dihydropyridine receptor II-III loop and partly structured 'C' region peptides modify cardiac ryanodine receptor activity. *Biochem. J. 385*, 803−813.
(10) Bers, D. M., and Stiffel, V. M. (1993) Ratio of ryanodine to dihydropyridine receptors in cardiac and skeletal muscle and implications for E-C coupling. *Am. J. Physiol. 264*, C1587−C1593.
(11) Franzini-Armstrong, C., Protasi, F., and Ramesh, V. (1998) Comparative ultrastructure of Ca^{2+} release units in skeletal and cardiac muscle. *Ann. N.Y. Acad. Sci. 853*, 20−30.
(12) Stern, M. D., and Cheng, H. (2004) Putting out the fire: What terminates calcium-induced calcium release in cardiac muscle? *Cell Calcium 35*, 591−601.
(13) Cannell, M. B., and Kong, C. H. (2012) Local control in cardiac E-C coupling. *J. Mol. Cell. Cardiol. 52*, 298−303.
(14) Stern, M. D. (1992) Theory of excitation-contraction coupling in cardiac muscle. *Biophys. J. 63*, 497−517.
(15) Wier, W. G., Egan, T. M., Lopez-Lopez, J. R., and Balke, C. W. (1994) Local control of excitation-contraction coupling in rat heart cells. *J. Physiol. 474*, 463−471.
(16) Cannell, M. B., Cheng, H., and Lederer, W. J. (1994) Spatial non-uniformities in $[Ca^{2+}]_i$ during excitation-contraction coupling in cardiac myocytes. *Biophys. J. 67*, 1942−1956.
(17) Lopez-Lopez, J. R., Shacklock, P. S., Balke, C. W., and Wier, W. G. (1994) Local, stochastic release of Ca^{2+} in voltage-clamped rat heart cells: Visualization with confocal microscopy. *J. Physiol. 480* (Part 1), 21−29.
(18) Cannell, M. B., Cheng, H., and Lederer, W. J. (1995) The control of calcium release in heart muscle. *Science 268*, 1045−1049.
(19) Santana, L. F., Cheng, H., Gomez, A. M., Cannell, M. B., and Lederer, W. J. (1996) Relation between the sarcolemmal Ca^{2+} current and Ca^{2+} sparks and local control theories for cardiac excitation-contraction coupling. *Circ. Res. 78*, 166−171.
(20) Hagalili, Y., Bachnoff, N., and Atlas, D. (2008) The voltage-gated Ca^{2+} channel is the Ca^{2+} sensor protein of secretion. *Biochemistry 47*, 13822−13830.
(21) El-Ani, D., Zimlichman, R., Mashiach, Y., and Shainberg, A. (2007) Adenosine and TNF-α exert similar inotropic effect on heart cultures, suggesting a cardioprotective mechanism against hypoxia. *Life Sci. 81*, 803−813.
(22) Shmist, Y. A., Kamburg, R., Ophir, G., Kozak, A., Shneyvays, V., Appelbaum, Y. J., and Shainberg, A. (2005) N,N,N′,N′-Tetrakis(2-pyridylmethyl)-ethylenediamine improves myocardial protection against ischemia by modulation of intracellular Ca^{2+} homeostasis. *J. Pharmacol. Exp. Ther. 313*, 1046−1057.
(23) Wiser, O., Trus, M., Hernandez, A., Renstrom, E., Barg, S., Rorsman, P., and Atlas, D. (1999) The voltage sensitive Lc-type Ca^{2+} channel is functionally coupled to the exocytotic machinery. *Proc. Natl. Acad. Sci. U.S.A. 96*, 248−253.
(24) Hohaus, A., Beyl, S., Kudrnac, M., Berjukow, S., Timin, E. N., Marksteiner, R., Maw, M. A., and Hering, S. (2005) Structural determinants of L-type channel activation in segment IIS6 revealed by a retinal disorder. *J. Biol. Chem. 280*, 38471−38477.
(25) Marom, M., Hagalili, Y., Sebag, A., Tzvier, L., and Atlas, D. (2010) Conformational changes induced in voltage-gated calcium channel Cav1.2 by BayK 8644 or FPL64176 modify the kinetics of secretion independently of Ca^{2+} influx. *J. Biol. Chem. 285*, 6996−7005.
(26) Cheng, H., Lederer, W. J., and Cannell, M. B. (1993) Calcium sparks: Elementary events underlying excitation-contraction coupling in heart muscle. *Science 262*, 740−744.
(27) Li, Y., and Bers, D. M. (2001) A cardiac dihydropyridine receptor II-III loop peptide inhibits resting Ca^{2+} sparks in ferret ventricular myocytes. *J. Physiol. 537*, 17−26.
(28) Nabauer, M., Callewaert, G., Cleemann, L., and Morad, M. (1989) Regulation of calcium release is gated by calcium current, not gating charge, in cardiac myocytes. *Science 244*, 800−803.
(29) Piacentino, V., III, Dipla, K., Gaughan, J. P., and Houser, S. R. (2000) Voltage-dependent Ca^{2+} release from the SR of feline ventricular myocytes is explained by Ca^{2+}-induced Ca^{2+} release. *J. Physiol. 523* (Part 3), 533−548.
(30) Trafford, A. W., and Eisner, D. A. (2003) No role for a voltage sensitive release mechanism in cardiac muscle. *J. Mol. Cell. Cardiol. 35*, 145−151.
(31) Kim, M. S., Morii, T., Sun, L. X., Imoto, K., and Mori, Y. (1993) Structural determinants of ion selectivity in brain calcium channel. *FEBS Lett. 318*, 145−148.
(32) Mikala, G., Bahinski, A., Yatani, A., Tang, S., and Schwartz, A. (1993) Differential contribution by conserved glutamate residues to an ion-selectivity site in the L-type Ca^{2+} channel pore. *FEBS Lett. 335*, 265−269.
(33) Tang, S., Mikala, G., Bahinski, A., Yatani, A., Varadi, G., and Schwartz, A. (1993) Molecular localization of ion selectivity sites within the pore of a human L-type cardiac calcium channel. *J. Biol. Chem. 268*, 13026−13029.
(34) Yang, J., Ellinor, P. T., Sather, W. A., Zhang, J. F., and Tsien, R. W. (1993) Molecular determinants of Ca^{2+} selectivity and ion permeation in L-type Ca^{2+} channels. *Nature 366*, 158−161.
(35) Ellinor, P. T., Yang, J., Sather, W. A., Zhang, J. F., and Tsien, R. W. (1995) Ca^{2+} channel selectivity at a single locus for high-affinity Ca^{2+} interactions. *Neuron 15*, 1121−1132.
(36) Cibulsky, S. M., and Sather, W. A. (2000) The EEEE locus is the sole high-affinity Ca^{2+} binding structure in the pore of a voltage-gated Ca^{2+} channel: Block by Ca^{2+} entering from the intracellular pore entrance. *J. Gen. Physiol. 116*, 349−362.
(37) Cloues, R. K., Cibulsky, S. M., and Sather, W. A. (2000) Ion interactions in the high-affinity binding locus of a voltage-gated Ca^{2+} channel. *J. Gen. Physiol. 116*, 569−586.
(38) Sather, W. A., and McCleskey, E. W. (2003) Permeation and selectivity in calcium channels. *Annu. Rev. Physiol. 65*, 133−159.
(39) Marom, M., Sebag, A., and Atlas, D. (2007) Cations residing at the selectivity filter of the voltage-gated Ca^{2+}-channel modify fusion-pore kinetics. *Channels 1*, 377−386.
(40) Atlas, D. (2010) Signaling role of the voltage-gated calcium channel as the molecular on/off-switch of secretion. *Cell. Signalling 22*, 1597−1603.
(41) Lerner, I., Trus, M., Cohen, R., Yizhar, O., Nussinovitch, I., and Atlas, D. (2006) Ion interaction at the pore of Lc-type Ca^{2+} channel is sufficient to mediate depolarization-induced exocytosis. *J. Neurochem. 97*, 116−127.
(42) Trus, M., Corkey, R. F., Nesher, R., Richard, A. M., Deeney, J. T., Corkey, B. E., and Atlas, D. (2007) The L-type voltage-gated Ca^{2+}

channel is the Ca^{2+} sensor protein of stimulus-secretion coupling in pancreatic β cells. *Biochemistry 46*, 14461−14467.
(43) Weiss, N. (2010) Control of depolarization-evoked presynaptic neurotransmitter release by Cav2.1 calcium channel: Old story, new insights. *Channels 4*, 431−433.
(44) Lockless, S. W., Zhou, M., and MacKinnon, R. (2007) Structural and thermodynamic properties of selective ion binding in a K^+ channel. *PLoS Biol. 5*, e121.
(45) Hess, P., Lansman, J. B., and Tsien, R. W. (1986) Calcium channel selectivity for divalent and monovalent cations. Voltage and concentration dependence of single channel current in ventricular heart cells. *J. Gen. Physiol. 88*, 293−319.
(46) Sham, J. S., Cleemann, L., and Morad, M. (1992) Gating of the cardiac Ca^{2+} release channel: The role of Na^+ current and Na^+-Ca^{2+} exchange. *Science 255*, 850−853.
(47) Cannell, M. B., Berlin, J. R., and Lederer, W. J. (1987) Intracellular calcium in cardiac myocytes: Calcium transients measured using fluorescence imaging. *Soc. Gen. Physiol. Ser. 42*, 201−214.
(48) Cannell, M. B., Berlin, J. R., and Lederer, W. J. (1987) Effect of membrane potential changes on the calcium transient in single rat cardiac muscle cells. *Science 238*, 1419−1423.
(49) Beuckelmann, D. J., and Wier, W. G. (1988) Mechanism of release of calcium from sarcoplasmic reticulum of guinea-pig cardiac cells. *J. Physiol. 405*, 233−255.
(50) Copello, J. A., Zima, A. V., Diaz-Sylvester, P. L., Fill, M., and Blatter, L. A. (2007) Ca^{2+} entry-independent effects of L-type Ca^{2+} channel modulators on Ca^{2+} sparks in ventricular myocytes. *Am. J. Physiol. 292*, C2129−C2140.
(51) Huang, G., Kim, J. Y., Dehoff, M., Mizuno, Y., Kamm, K. E., Worley, P. F., Muallem, S., and Zeng, W. (2007) Ca^{2+} signaling in microdomains: Homer1 mediates the interaction between RyR2 and Cav1.2 to regulate excitation-contraction coupling. *J. Biol. Chem. 282*, 14283−14290.
(52) Isenberg, G., and Han, S. (1994) Gradation of Ca^{2+}-induced Ca^{2+} release by voltage-clamp pulse duration in potentiated guinea-pig ventricular myocytes. *J. Physiol. 480* (Part 3), 423−438.
(53) Cleemann, L., and Morad, M. (1991) Role of Ca^{2+} channel in cardiac excitation-contraction coupling in the rat: Evidence from Ca^{2+} transients and contraction. *J. Physiol. 432*, 283−312.
(54) Ferrier, G. R., and Howlett, S. E. (1995) Contractions in guinea-pig ventricular myocytes triggered by a calcium-release mechanism separate from Na^+ and L-currents. *J. Physiol. 484* (Part 1), 107−122.